

Dynamically induced two-color nonreciprocity in a tripod system of a moving atomic latticeLiu Yang,^{1,2} Yan Zhang,^{2,3,*} Xiao-Bo Yan,⁴ Ying Sheng,¹ Cui-Li Cui,^{1,†} and Jin-Hui Wu^{2,3}¹College of Physics, Jilin University, Changchun 130023, People's Republic of China²Center for Quantum Sciences, Northeast Normal University, Changchun 130117, People's Republic of China³School of Physics, Northeast Normal University, Changchun 130024, People's Republic of China⁴Institute of Theoretical Physics, Chinese Academy of Sciences, Beijing 100190, People's Republic of China

(Received 28 May 2015; published 30 November 2015)

We study the two-color nonreciprocal effects of transmission and reflection in cold atoms driven into the tripod configuration and confined in a moving optical lattice. Our numerical results show that a very high contrast of the forward-backward transmission up to around 92% (reflection up to around 85%) is observable near the sharp edges of two tunable photonic band gaps at lattice speeds of several meters per second. Such two-color optical nonreciprocity is attained in fact by breaking the time-reversal symmetry with asymmetric Doppler shifts and can be dynamically manipulated by varying the driving and coupling field detunings, the probe pulse length, the atomic lattice velocity, etc.

DOI: [10.1103/PhysRevA.92.053859](https://doi.org/10.1103/PhysRevA.92.053859)

PACS number(s): 42.50.Gy, 42.50.Wk, 37.10.Vz, 42.70.Qs

I. INTRODUCTION

In the past few decades, much attention has been paid to the study of electromagnetically induced transparency (EIT) [1–3], a quantum interference effect induced by a strong coupling field, based on which the optical absorption of a weak probe field can be largely suppressed in a small frequency range while the large-dispersion property remains. Electromagnetically induced transparency has many important applications, such as slow light [4,5], quantum memory [6–9], and nonlinearity enhancement [10,11]. It is well known that the photonic band gaps (PBG) of a traditional photonic crystal (PC) cannot be modulated because the periodic structure is determined once a PC is grown. Recently, the tunable PBG generated in cold atoms loaded in an optical lattice under EIT conditions has achieved spectacular progress [12–14]. Petrosyan's work [12] showed that a new band gap may arise within the transparent window, which is very narrow and dynamically tunable. Then Schilke *et al.* investigated experimentally the Bragg reflection, reported the measurements of transmission and reflection spectra and their dependence on the experimental parameters, and discussed the limitations of this system [15,16]. Recently, the study of optical nonreciprocity with controlled PBGs has attracted a great deal of interest [17,18].

Generally, it is hard to achieve nonreciprocity in the familiar process of linear reflection and transmission of light [19], which, however, can be engineered to develop advanced materials and functional composite systems. Thus, great effort has been made to achieve optical nonreciprocity recently, such as using media with parity-time (\mathcal{PT}) symmetry [20–29], media with acousto-optical effects [30] or magneto-optical effects [31], and nonsymmetric photonic crystals [32]. In particular, \mathcal{PT} -symmetric periodic structures may exhibit reflection nonreciprocity near the spontaneous \mathcal{PT} -symmetry breaking point, i.e., an imbalance between the forward and backward reflectivities [22]. Recently, it was found that the nonreciprocal transmission can be achieved by setting the

photonic crystal [17] and periodically distributed atoms [18] into motion. When a photonic crystal moves, the counter-propagating light is blueshifted and the copropagating light is redshifted in the reference frame of the moving photonic crystal due to the Doppler effect [18]. Because of the difficulty of realizing the moving photonic crystal, they rendered the optically induced photonic crystal moving in the static EIT medium by slightly detuning the two counterpropagating components of the standing-wave field [17]. Optical nonreciprocity has been proposed for the realization of all-optical diodes [33–35] and unidirectional light transport [36].

In this paper we extend the work [18] and study the two-color nonreciprocal effect of transmission and reflection in a moving cold atomic lattice driven into a four-level tripod configuration. It should be noted that, in this paper, the one-dimensional (1D) PBGs are formed by cold atoms trapped in a 1D lattice as shown in [15] and this system may create two new PBGs. We discuss in detail how the cold atoms move at speeds of several meters per second and report that the incident probe pulse propagating along the optical lattice can be controlled and experience high nonreciprocal transmission and reflection (namely, obvious forward-backward asymmetry in transmission and reflection) within two frequency regions corresponding, respectively, to the sharp edges of the two new PBGs. Compared with previous work, we choose a more reasonable atomic density distribution and a lower atomic speed of 3 m/s in the optical lattice, which has been investigated experimentally [37]. We also analyze the density of states (DOS) for probe photons, which is further evidence of the existence of optical nonreciprocity. In addition, it is discussed that the degree and frequency regions of the nonreciprocity could be controlled by varying the driving and coupling field detunings, the probe pulse length, the atomic lattice velocity, etc.

II. THEORETICAL MODEL AND EQUATIONS

As shown in Fig. 1(a), we study a four-level tripod atomic system where levels $|0\rangle$, $|1\rangle$, $|2\rangle$, and $|3\rangle$ correspond to states $|5S_{1/2}, F=2, m=-2\rangle$, $|5S_{1/2}, F=1, m=0\rangle$, $|5S_{1/2}, F=1, m=-1\rangle$, and $|5P_{3/2}, F=2, m=-1\rangle$ of ^{87}Rb atoms, respectively. A static magnetic field is applied to break the

*Corresponding author: zhangy345@nenu.edu.cn

†Corresponding author: cuiculi@jlu.edu.cn

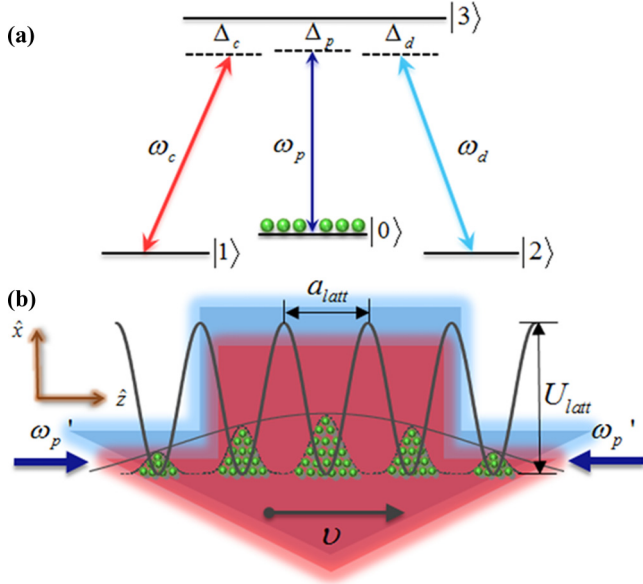


FIG. 1. (Color online) (a) Energy-level diagram form of a four-level tripod-type atomic system interacting with a probe field ω_p , a coupling field ω_c , and a driving field ω_d . (b) Atoms are trapped in an optical lattice formed by a retroreflecting laser beam of wavelength λ_{latt} that is far detuned from relevant atomic resonances. The confined atoms are located at the standing-wave antinodes of period $a_{\text{latt}} = \lambda_{\text{latt}}/2$. The probe is assumed to travel in the z direction and the coupling and driving fields propagate in the x direction. The periodic multilayer structure is set to move with a constant velocity v along its optical axis \hat{z} .

degeneracy of levels $|1\rangle$ and $|2\rangle$. The atomic transition between level $|3\rangle$ and level $|0\rangle$, $|1\rangle$, or $|2\rangle$ is coherently driven by a probe, coupling, or driving field propagating in the \hat{z} , \hat{x} , or \hat{x} direction with σ^+ , σ^- , or π polarization, respectively. The probe field ω_p is detuned from the atomic transition $|3\rangle \rightarrow |0\rangle$ by $\Delta_p = \omega_{30} - \omega_p$, the coupling field ω_c is detuned from the atomic transition $|3\rangle \rightarrow |1\rangle$ by $\Delta_c = \omega_{31} - \omega_c$, and the driving field ω_d is detuned from atomic transition $|3\rangle \rightarrow |2\rangle$ by $\Delta_d = \omega_{32} - \omega_d$.

Under the electric dipole and rotating-wave approximations, the interaction Hamiltonian can be rewritten as

$$H(t) = -\hbar \begin{bmatrix} 0 & 0 & 0 & \Omega_p^* \\ 0 & \Delta_p - \Delta_c & 0 & \Omega_c^* \\ 0 & 0 & \Delta_p - \Delta_d & \Omega_d^* \\ \Omega_p & \Omega_c & \Omega_d & \Delta_p \end{bmatrix}, \quad (1)$$

from which it is straightforward to attain 16 dynamic equations for the mutually coupled density-matrix elements ρ_{hk} with $h, k \in \{1, 2, 3, 4\}$.

In the weak probe limit, the above density-matrix equations can be reduced to

$$\begin{aligned} \partial_t \rho_{10} &= -[\gamma_{10} - i(\Delta_p - \Delta_c)]\rho_{10} + i\Omega_c^* \rho_{30}, \\ \partial_t \rho_{20} &= -[\gamma_{20} - i(\Delta_p - \Delta_d)]\rho_{20} + i\Omega_d^* \rho_{30}, \\ \partial_t \rho_{30} &= -[\gamma_{30} - i\Delta_p]\rho_{30} + i\Omega_c \rho_{10} + i\Omega_d \rho_{20} + i\Omega_p, \end{aligned} \quad (2)$$

as we assume that $\rho_{00} = 1$, $\rho_{11} = \rho_{22} = \rho_{33} = 0$, and $\rho_{21} = \rho_{31} = \rho_{32} = 0$ without introducing notable errors. Here γ_{hk} is

the decay rate of atomic coherence for the transition $|h\rangle \leftrightarrow |k\rangle$. Thus we can solve Eq. (2) analytically in the steady state ($\partial_t \rho_{hk} = 0$) to obtain the probe susceptibility

$$\begin{aligned} \chi_p(z) &= \frac{N(z)|d_{03}|^2 \rho_{30}}{2\epsilon_0 \hbar \Omega_p} \\ &= \frac{N(z)|d_{03}|^2}{2\epsilon_0 \hbar} \frac{i\gamma'_{10}\gamma'_{20}}{\gamma'_{10}\gamma'_{20}\gamma'_{30} + \gamma'_{10}\Omega_d^2 + \gamma'_{20}\Omega_c^2}, \end{aligned} \quad (3)$$

where $\gamma'_{10} = \gamma_{10} - i(\Delta_p - \Delta_c)$, $\gamma'_{20} = \gamma_{20} - i(\Delta_p - \Delta_d)$, and $\gamma'_{30} = \gamma_{30} - i\Delta_p$ are the complex dephasing rates and $N(z)$ is the inhomogeneous atomic density as a function of the lattice position z .

These cold ^{87}Rb atoms are trapped in a standing-wave dipole trap, which is used to store any desired small number of cold atoms, formed by a red-detuned retroreflected laser beam of wavelength λ_{latt} [see Fig. 1(b)]. The temperature T_0 of the inhomogeneous atomic sample is usually related to the trapping depth U_{latt} of the optical potential by a constant factor $\eta = U_{\text{latt}}/k_B T_0$ (where k_B is the Boltzmann constant). The laser forming the lattice must have a wavelength $\lambda_{\text{latt}} > \lambda_{30}$ to generate the dipole traps. This means that the Bragg condition can only be fulfilled with a nonzero propagation angle θ between the probe and the lattice beams, which should be small enough so that the probe interacts with the lattice over its entire length. From the geometric Bragg condition $\lambda_0 = \lambda_{30}/\cos\theta$, we can thus define $\Delta\lambda_{\text{latt}} = \lambda_{\text{latt}} - \lambda_0$ as the shift. It is also worth noting that the inhomogeneous sample density has a big Gaussian profile [see Fig. 1(b)], which is quite typical for cold atomic clouds in a magneto-optical trap [38] and can be defined by $N_L(z) \propto \exp[-20(z - L/2)^2/L^2]$, with L being the length of lattice [39], while each dipole-trap period of the optical lattice exhibits a small Gaussian density distribution $N_d(z) \propto 1/\sqrt{2\pi}\sigma_z \exp[-(z - z_i - a_{\text{latt}}/2)^2/2\sigma_z^2]$ with an rms width $\sigma_z = \lambda_{\text{latt}}/2\pi\sqrt{2\eta}$ along the lattice axis \hat{z} , $z_i = (i - 1/2)a_{\text{latt}}$ being the central position of the i th period along \hat{z} ($i = 1, 2, \dots, n$) and $a_{\text{latt}} = L/n$ being the length of each period. Then the density distribution of the whole sample $N(z)$ should be expressed by a piecewise function, which has n pieces. The i th piece is $N_i(z) = N' \exp[-(z - z_i - a_{\text{latt}}/2)^2/2\sigma_z^2] \exp[-20(z_i - L/2)^2/L^2]$, with $N' = \alpha N_{\text{av}}$ and N_{av} being the average atomic density, where the constant factor α can be determined by $N_{\text{av}}L = \sum_{i=1}^n \int_{-a_{\text{latt}}/2}^{a_{\text{latt}}/2} N_i(z) dz$.

In this atomic sample, the probe field may experience three PBGs, which can be verified by utilizing the transfer-matrix method [40]. In brief, the first step is to construct a transfer matrix M_j of the j th single period, which should be decomposed into, e.g., 100 sublayers of the same thickness $\delta_z (\ll a_{\text{latt}})$ but of different atomic densities $N(z_l)$ with ($l \in 1, 100$). The transfer matrix $m_j(z_l)$ of each sublayer is the product of a propagation matrix with a discontinuity matrix whose coefficients are given by the Fresnel coefficients (see [41]) and is related to the elementary reflection and transmission coefficients r_j and t_j as

$$m_j(z_l) = \frac{1}{t_j(z_l)} \begin{bmatrix} t_j^2(z_l) - r_j^2(z_l) & r_j(z_l) \\ -r_j(z_l) & 1 \end{bmatrix}. \quad (4)$$

Then $M_j = m_j(z_1) \cdots m_j(z_l) \cdots m_j(z_{100})$. The second step is to attain the transfer matrix M for the whole atomic

sample of length $L = na_{\text{latt}}$. Since the inhomogeneous sample density distribution is not the same in each dipole-trap period as we have analyzed in the preceding paragraph [also see Fig. 1(b)], $M \neq M_j^n$. We should multiply transfer matrices of all partitioned periods to attain the total transfer matrix $M = M_1 \cdots M_j \cdots M_n$. Then it is easy to calculate the probe reflectivities and transmissivities

$$R_n = \left| \frac{M_{(12)}}{M_{(22)}} \right|^2, \quad T_n = \left| \frac{1}{M_{(22)}} \right|^2, \quad (5)$$

with $M_{(ij)}$ being one matrix element of the total transfer matrix M .

In addition, we note that PBGs can also be examined by the sufficiently reduced DOS for probe photons. This can be calculated by following the method in Ref. [15] via

$$\mathcal{D}(z) = \text{Re} \left[\frac{2 + r_l(z) + r_r(z)}{1 - r_l(z)r_r(z)} - 1 \right] \quad (6)$$

normalized to the free-space DOS. In Eq. (6), r_l and r_r are the complex reflection coefficients experienced by photons ω_p emitting to, respectively, the left and right ends of the 1D atomic lattice from position z .

In the rest frame, the frequency-dependent reflectivity $\mathcal{R}(\omega)$ and transmissivity $\mathcal{T}(\omega)$ are reciprocal. However, in the laboratory frame [as shown in Fig. 1(b), the optical lattice is set to move with a constant velocity v along its optical axis \hat{z}], at a given incident frequency ω' , the transmissivities $\mathcal{T}(\omega')$ and reflectivities $\mathcal{R}(\omega')$ are different between the two propagation directions $+\hat{z}$ and $-\hat{z}$ since the Doppler effect gives rise to two different rest frame frequencies. Generally, for a Gaussian pulse of central frequency ω'_p and spatial length \mathcal{L}' propagating through the moving multilayer along $+\hat{z}$ or $-\hat{z}$, the corresponding laboratory frame reflectivity and transmissivity need to be written as [18]

$$R_{\pm}(\omega'_p) \simeq \frac{\mathcal{L}'}{c\sqrt{2\pi}} \int_{-\infty}^{\infty} d\omega' e^{-[(\omega' - \omega'_p)^2/2(c/\mathcal{L}')^2]} \times \mathcal{R}((1 \mp v/c)\omega'), \quad (7)$$

$$T_{\pm}(\omega'_p) \simeq \frac{\mathcal{L}'}{c\sqrt{2\pi}} \int_{-\infty}^{\infty} d\omega' e^{-[(\omega' - \omega'_p)^2/2(c/\mathcal{L}')^2]} \times \mathcal{T}((1 \mp v/c)\omega'). \quad (8)$$

As expected from the Doppler effect, the band gaps experienced by the forward and backward monochromatic light of frequency ω' are shifted by $\mp\omega'(v/c)$. Here the multilayer structure we consider has a smooth frequency dependence of the reflectivity and transmissivity over the pulse bandwidth c/\mathcal{L}' . Thus, forward-backward asymmetry in pulse transmission and reflection can be characterized by the nonreciprocity parameters $\Delta T(\omega'_p) = T_+(\omega'_p) - T_-(\omega'_p)$ and $\Delta R(\omega'_p) = R_+(\omega'_p) - R_-(\omega'_p)$, which can be calculated by expanding \mathcal{T} and \mathcal{R} in Taylor series [18]

$$\Delta T(\omega'_p) \approx -v/c \{ 2\omega'_p [d\mathcal{T}(\omega'_p)/d\omega] + (2c/\mathcal{L}')^2 \times [d^2\mathcal{T}(\omega'_p)/d\omega^2] \}, \quad (9)$$

$$\Delta R(\omega'_p) \approx -v/c \{ 2\omega'_p [d\mathcal{R}(\omega'_p)/d\omega] + (2c/\mathcal{L}')^2 \times [d^2\mathcal{R}(\omega'_p)/d\omega^2] \}. \quad (10)$$

This means that for a nearly monochromatic pulse ($\mathcal{L}' \rightarrow \infty$), an appreciable degree of transmission or reflection nonreciprocity would require a sharp frequency derivative $|dT(\omega)/d\omega|$ or $|d\mathcal{R}(\omega)/d\omega|$, respectively.

III. RESULTS AND DISCUSSION

As expected from the Doppler effect, the optical response of a moving atom will be changed. The main manifestation is that the probe susceptibility will experience a frequency shift along the direction of motion. As the effects of a single atom on the probe propagation could be neglected, unless the probe field is on the single-photon level, a moving homogeneous atomic ensemble should be further considered. The probe transmissivity and absorption coefficient of the moving atomic ensemble will be changed due to the Doppler frequency shift experienced by the probe susceptibility. Then, if the forward-incident probe frequency is within the EIT window, the backward-incident frequency may be located at the absorption peak, which will give rise to forward-backward nonreciprocity in probe transmission and absorption. For a moving atomic lattice, the probe transmissivity and reflectivity will be changed due to the existence of PBGs and their Doppler frequency shifts. This will give rise to forward-backward nonreciprocity in probe transmission and reflection. By controlling the corresponding parameters properly, the full reflection in one direction and full transmission in the other direction can be achieved simultaneously.

In this section we explore, via full numerical calculations, how to generate and manipulate two-color nonreciprocal reflection and transmission in the coherently driven atomic lattice in terms of the pulse reflectivity and transmissivity, the pulse nonreciprocity parameter, and the density of photonic states. We first examine the probe reflectivity and transmissivity profiles in the rest frame. As shown in Fig. 2(a), three PBGs may appear as three high reflection platforms R_1 , R_2 , and R_3 . The highlighted sharp edges of the first two PBGs R_1 and R_2 , which are contributed by the coupling and driving fields, are useful to obtain the large nonreciprocal effects for a nearly monochromatic pulse with a full bandwidth of 1.0 MHz ($\mathcal{L}' = 300$ m). Meanwhile, two transmission peaks T_1 and T_2 with sharp edges are also attained as shown in Fig. 2(b).

In this system, the far-detuned standing-wave dipole trap is formed by two counterpropagating laser beams with equal intensities and optical frequencies ν_1 and ν_2 , which produces a position-dependent dipole potential $U(z, t) = U_{\text{latt}} \cos^2[\pi(\Delta\nu t - 2z/\lambda_{\text{latt}})]$, where z is the position of the atoms and $\Delta\nu$ is the frequency difference of two beams. Two independent acousto-optic modulators control the value of $\Delta\nu$ producing an optical lattice moving at velocity $v = \lambda\Delta\nu/2$. The depth of the optical dipole trap can be written as $U_{\text{latt}} = n_0 E_R$, where n_0 depends on units of the recoil energy $E_R = \hbar^2 k^2/2m$. The typical kinetic energy of the trapped atom is considerably smaller than the trap depth, so the atoms could avoid running away from the dipole trap. By controlling the motion of the standing wave, the atoms can be transported with a constant velocity of several meters per second. In Ref. [37] the atoms could be accelerated from 0 to 10 m/s in 100 μ s with a constant transportation efficiency of more than 95%.

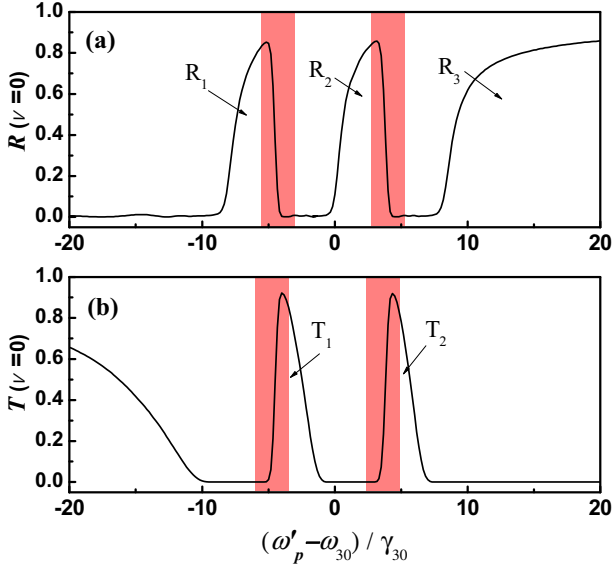


FIG. 2. (Color online) Rest frame (a) reflectivity and (b) transmissivity for an atomic Bragg mirror with inhomogeneous atomic density $N(z)$. Other parameters are $L' = 300$ m, $\gamma_{30} = \gamma_{31} = \gamma_{32} = \gamma = 6$ MHz, $\gamma_{01} = \gamma_{02} = 0.008\gamma$, $\Omega_c = \Omega_d = 5\gamma$, $\Delta_c = -\Delta_d = 4.2\gamma$, $N_{av} = 2.0 \times 10^{12}$ cm $^{-3}$, $\mu_{03} = 1.0 \times 10^{-29}$ C m, $\lambda_{\text{latt}} = 794.983$ nm, $\lambda_{30} = 794.969$ nm, $\Delta\lambda_{\text{latt}} = 0.25$ nm, $\eta = 3.5$, and $L = 3.0$ mm.

In the following we will examine the optical response of our system in the laboratory frame.

In Fig. 3 we show the forward-backward asymmetry in reflection and transmission according to the nonreciprocity parameters $\Delta R(\omega'_p) \equiv R_+(\omega'_p) - R_-(\omega'_p)$ and $\Delta T(\omega'_p) \equiv$

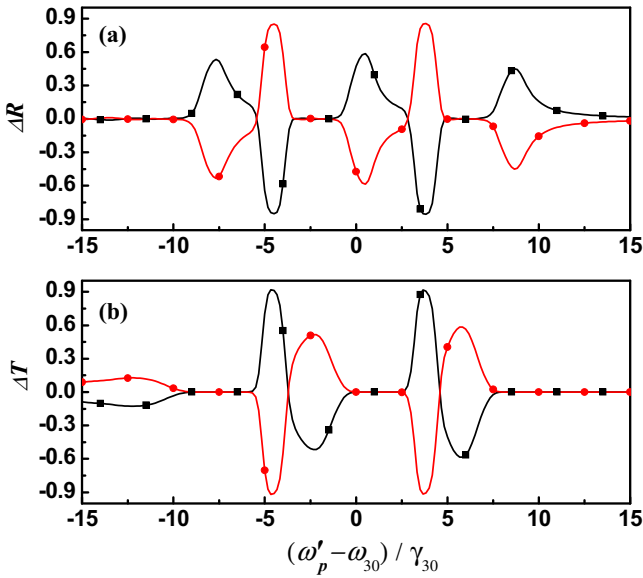


FIG. 3. (Color online) (a) Reflection nonreciprocity parameter ΔR_p and (b) transmission nonreciprocity parameter ΔT_p as functions of the detuning of the probe central frequency ω'_p from the atomic resonance ω_{30} computed with $v = -3$ m/s (black line with squares) or $v = 3$ m/s (red line with circles). Other parameters are the same as in Fig. 2.

$T_+(\omega'_p) - T_-(\omega'_p)$. As we can see, two large nonreciprocity parameters appear within two frequency regions that correspond, respectively, to the two sharp edges of PBGs R_1 and R_2 highlighted in Fig. 2. The two transmission (reflection) nonreciprocity peaks $|\Delta T_1| \approx |\Delta T_2|$ ($|\Delta R_1| \approx |\Delta R_2|$) may reach around 92% (85%), even at speeds as slow as 3 m/s. This means that within these two frequency regions, the incident probe pulse can be transmitted almost totally in one direction but not in the other direction (reflected totally in the other direction). Changing the sign of v (reversing the motion of the atomic lattice) would change the signs of the two-color reflection and transmission nonreciprocity parameters. It is worth noting that the existence of PBGs and motion-induced nonreciprocity are not unique to this trapped atomic gas setup. The similar nonreciprocal effects can also be achieved, for example, by using the traditional moving photonic crystal, but the nonreciprocal output is low since the edges of PBGs are not sharp enough. However, in our scheme, the nonreciprocity can be enhanced by using laser-induced quantum interference. The underlying physical reason is that deeply narrow EIT windows can be generated by using laser-induced quantum interference. This will further give rise to narrow PBGs with sufficiently sharp edges, which is the key to high nonreciprocal output [see Eqs. (9) and (10)]. Finally, we note that the peak transmission (reflection) nonreciprocity will reduce to around 56% (68%) if the ratios between two-photon and one-photon decay rates (γ_{01}/γ and γ_{02}/γ) are increased by one order of magnitude from their current values, keeping all other system parameters constant. This nonreciprocity reduction, however, can be compensated for by properly choosing other parameters, e.g., Rabi frequencies of the coupling and driving fields, to narrow down the EIT windows.

In Fig. 4 we plot the local density of photonic states $D_{\pm}(z)$ with the probe central frequency ω'_p within the sharp edge of the first PBG R_1 as a function of the lattice position z . Here + and - correspond to a probe pulse propagating forward ($+\hat{z}$) and backward ($-\hat{z}$), respectively. As we can see, $D_+(z)$

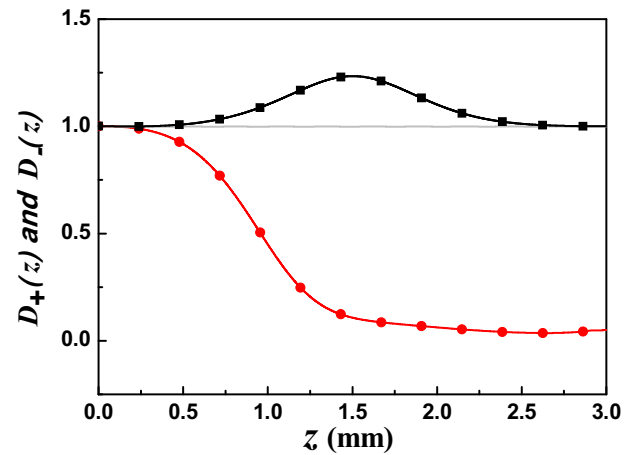


FIG. 4. (Color online) Density of states $D_+(z)$ (red line with circles) and $D_-(z)$ (black line with squares) as functions of atomic lattice position z computed for $(\omega'_p - \omega_{30})/\gamma = -4.6$ and $v = 3$ m/s. The gray line corresponds to a homogeneous atomic medium of the same average density $N_{av} = 2.0 \times 10^{12}$ cm $^{-3}$. Other parameters are the same as in Fig. 2.

decreases gradually from 1 to nearly 0 when it is integrated over the lattice length, while $D_-(z)$ increases from 1 at first and then decreases back to nearly 1 again when it is integrated over the lattice length. This means that when the atomic lattice moves in the forward direction $+\hat{z}$, the density distribution of the probe field propagating forward $(+\hat{z})$ through the atomic lattice will decrease gradually and become nearly zero at the sample's exit, while the one of the probe field propagating backward $(-\hat{z})$ through the atomic lattice will attain the nearly the same value at the sample's exit. In other words, the probe field propagating forward will almost not get out of the moving atomic lattice, while the one propagating backward will almost get out totally. The underlying physics is that, due to the Doppler effect, the band gaps experienced by the forward and backward probe fields with central frequency ω'_p [$(\omega'_p - \omega_{30})/\gamma = -4.6$] are shifted by $\mp\omega'_p(v/c)$. Namely, the forward probe field will experience a band gap R_1 , while the backward probe field will experience a transmission peak T_1 (see Fig. 2). Note that $D_-(z)$ increases at first and then decreases when it is integrated over the lattice length and attains the largest value in the lattice center. The underlying physics is the slow light propagation. The group velocity of a probe field in an EIT medium is ultraslow and inversely proportional to the atomic density. In this work the inhomogeneous sample density has a similar Gaussian profile [see Fig. 1(b)]. Thus, the group velocity of the probe field will get slower when the probe field penetrates deeply into the center of the lattice. Then more probe photons will be found in the center of the lattice. The DOS with the probe central frequency within the sharp edge of the second PBG R_2 has the same profile as the one with the probe central frequency within the sharp edge of the first PBG R_1 and is not shown here. This is further evidence of the existence of two-color reflection (transmission) nonreciprocity.

In Fig. 5 we analyze the relationship between the frequency regions of the nonreciprocity parameter ΔR (ΔT) with the detunings Δ_c and Δ_d . As the absolute values of detunings $\Delta_c/\gamma_{30} = -\Delta_d/\gamma_{30}$ decrease, the two frequency regions of the nonreciprocity peaks become close. The underlying physics is that the PBGs will appear within the two resonant transparent windows whose positions depend on the coupling and driving detunings Δ_c and Δ_d . In particular, when $\Delta_c = \Delta_d = 0$, only one frequency region with very large nonreciprocal effects may exist within the single degenerated transparent window.

In Fig. 6 we further show the dependence of the absolute value of the nonreciprocity parameter $|\Delta R_1|$ ($|\Delta T_1|$) on the pulse length \mathcal{L}' and sample velocity v , respectively. The parameter ΔR_2 (ΔT_2) is not shown here since $\Delta R_2 \approx \Delta R_1$ ($\Delta T_2 \approx \Delta T_1$) with these parameters. Figure 6(a) shows that both $|\Delta T_1|$ and $|\Delta R_1|$ will be enhanced monotonically with increasing pulse length \mathcal{L}' . Specifically, they increase quickly when $\mathcal{L}' < 180$ m, change slowly when $\mathcal{L}' > 180$ m, and remain invariant when $\mathcal{L}' > 300$ m. Figure 6(b) shows that both $|\Delta T_1|$ and $|\Delta R_1|$ are enhanced monotonically when the sample velocity v is increased. Specifically, they increase quickly when $v < 2.5$ m/s, change slowly when $v > 2.5$ m/s, and keep invariant when $v > 3$ m/s. Thus, both the two-color nonreciprocal reflection and nonreciprocal transmission can be manipulated by modulating the pulse length \mathcal{L}' and the sample velocity v properly.

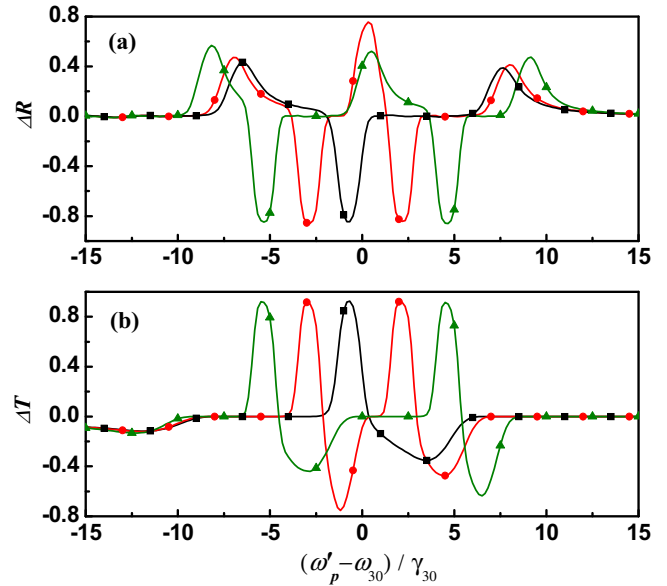


FIG. 5. (Color online) (a) Reflection nonreciprocity parameter ΔR and (b) transmission nonreciprocity parameter ΔT as functions of the normalized probe detuning $(\omega'_p - \omega_{30})/\gamma$ computed for $v = -3$ m/s with $\Delta_c/\gamma = -\Delta_d/\gamma = 5$ (green line with triangles), 2.5 (red line with circles), and 0 (black line with squares). Other parameters are the same as in Fig. 2.

Finally, it is worth noting that any level configuration that leads to double EIT windows can in principle give rise to two PBGs in an atomic lattice, which further allow for the emergence of similar two-color nonreciprocity due to the Doppler effect. However, the nonreciprocal effect depends on

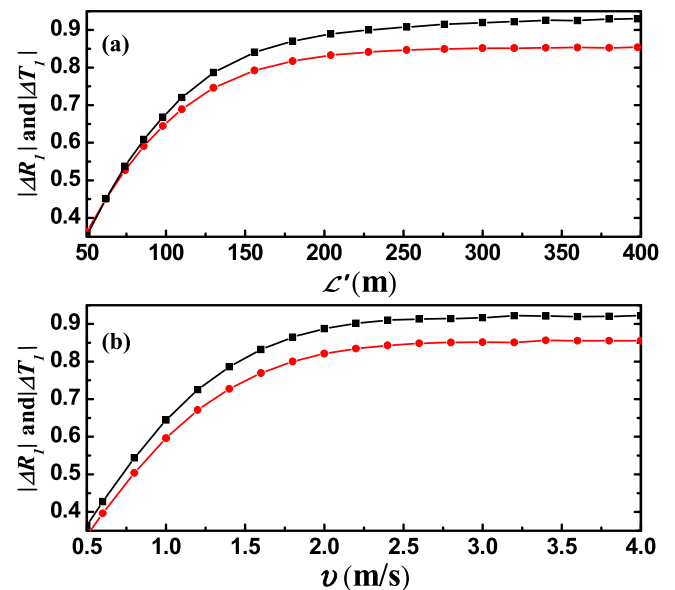


FIG. 6. (Color online) (a) Absolute value of pulse nonreciprocity parameters $|\Delta T_1|$ (black line with squares) and $|\Delta R_1|$ (red line with circles) as functions of \mathcal{L}' computed for $v = 3$ m/s. (b) Absolute value of pulse nonreciprocity parameters $|\Delta T_1|$ (black line with squares) and $|\Delta R_1|$ (red line with circles) as functions of v computed for $\mathcal{L}' = 300$ m. Other parameters are the same as in Fig. 2.

whether the EIT windows are narrow enough and whether the edges of the PBGs are sharp enough. The tripod configuration we considered here is the simplest and most available one to obtain double EIT windows, which can lead to PBGs with edges sharp enough under proper parameter conditions. Thus it can be used to achieve the ideal two-color nonreciprocity. Also note that the detunings of both control fields have been set to have opposite signs in this work. Actually, this is not a required condition. In principle, as long as the detunings of both control fields are different, two (nondegenerate) EIT windows will appear in different frequency ranges and two (nondegenerate) PBGs will be observed. However, it should be noted that the detunings cannot be too large so as to weaken the effective coupling between the control field and the atoms. The nonreciprocity experienced by the probe field will arise within the frequency regions where the PBGs exist, namely, where the two-photon resonant conditions between the probe and coupling fields are satisfied. The nonreciprocity has no direct relationship to whether the detunings of both control fields have opposite signs or not. The reason for this parameter setting is just that we expect to show basically symmetric spectra and to make the figures much more refined.

IV. CONCLUSION

In summary, we have discussed the two-color transmission and reflection nonreciprocity of a moving optical lattice with an inhomogeneous Gaussian atomic density distribution. We

found that two-color nonreciprocal effects with a high degree can be attained in two spectral regions, which can be characterized by large reflection and transmission nonreciprocity parameters and large differences between densities of photonic states in two counterpropagating directions. The degree and frequency regions of the nonreciprocal effects could be easily controlled by modulating the frequencies of coupling and driving fields, the velocity of the cold atoms, and the probe pulse lengths. The transmission nonreciprocity can be used to produce optical diodes or optical isolators, while the reflection nonreciprocity can be used to design invisible metamaterials, such as those absorbing the electromagnetic waves emitted from radar to minimize the corresponding reflection and scattering. The technique shown here could be easily extended to other multilevel systems with multicolor nonreciprocal effects.

ACKNOWLEDGMENTS

This work was supported by the National Basic Research Program of China (Grant No. 2011CB921603), the National Natural Science Foundation of China (Grants No. 11174110, No. 11247005, and No. 61378094), the Basic Scientific Research Funds of Jilin University, the Fundamental Research Funds for the Central Universities (Grant No. 12QNJJ006), the China Postdoctoral Science Foundation (Grant No. 2013T60316), and the Jilin Post Doctorate Science Research Program (Program No. RB201330).

-
- [1] S. E. Harris, *Phys. Today* **50**(7), 36 (1997).
 - [2] M. Fleischhauer, A. Imamoglu, and J. P. Marangos, *Rev. Mod. Phys.* **77**, 633 (2005).
 - [3] Y. Zhang, J.-W. Gao, C.-L. Cui, Y. Jiang, and J.-H. Wu, *Phys. Lett. A* **374**, 1088 (2010).
 - [4] L. V. Hau, S. E. Harris, Z. Dutton, and C. H. Behroozi, *Nature (London)* **397**, 594 (1999).
 - [5] M. M. Kash, V. A. Sautenkov, A. S. Zibrov, L. Hollberg, G. R. Welch, M. D. Lukin, Y. Rostovtsev, E. S. Fry, and M. O. Scully, *Phys. Rev. Lett.* **82**, 5229 (1999).
 - [6] C. Liu, Z. Dutton, C. H. Behroozi, and L. V. Hau, *Nature (London)* **409**, 490 (2001).
 - [7] Y. W. Cho and Y. H. Kim, *Phys. Rev. A* **82**, 033830 (2010).
 - [8] Y. Zhang, Y. Zhang, X.-H. Zhang, M. Yu, C.-L. Cui, and J.-H. Wu, *Phys. Lett. A* **376**, 656 (2012).
 - [9] Q.-Y. He, M. D. Reid, E. Giacobino, J. Cviklinski, and P. D. Drummond, *Phys. Rev. A* **79**, 022310 (2009).
 - [10] H. Schmidt and A. Imamoglu, *Opt. Lett.* **21**, 1936 (1996).
 - [11] S. H. Asadpour, M. Sahrai, A. Soltani, and H. R. Hamedi, *Phys. Lett. A* **376**, 147 (2012).
 - [12] D. Petrosyan, *Phys. Rev. A* **76**, 053823 (2007).
 - [13] H. Yang, L. Yang, X.-C. Wang, C.-L. Cui, Y. Zhang, and J.-H. Wu, *Phys. Rev. A* **88**, 063832 (2013).
 - [14] Y. Zhang, Y.-M. Liu, X.-D. Tian, T.-Y. Zheng, and J.-H. Wu, *Phys. Rev. A* **91**, 013826 (2015).
 - [15] A. Schilke, C. Zimmermann, and W. Guerin, *Phys. Rev. A* **86**, 023809 (2012).
 - [16] A. Schilke, C. Zimmermann, P. W. Courteille, and W. Guerin, *Phys. Rev. Lett.* **106**, 223903 (2011).
 - [17] D.-W. Wang, H.-T. Zhou, M.-J. Guo, J. X. Zhang, J. Evers, and S.-Y. Zhu, *Phys. Rev. Lett.* **110**, 093901 (2013).
 - [18] S. A. R. Horsley, J.-H. Wu, M. Artoni, and G. C. La Rocca, *Phys. Rev. Lett.* **110**, 223602 (2013).
 - [19] P. Yeh, *Optical Waves in Layered Media* (Wiley-Interscience, New York, 2005).
 - [20] S. Longhi, *Phys. Rev. A* **82**, 031801 (2010).
 - [21] C. E. Rüter, K. G. Makris, R. El-Ganainy, D. N. Christodoulides, M. Segev, and D. Kip, *Nat. Phys.* **6**, 192 (2010).
 - [22] L. Feng, Y.-L. Xu, W. S. Fegadolli, M.-H. Lu, J. E. B. Oliveira, V. R. Almeida, Y.-F. Chen, and A. Scherer, *Nat. Mater.* **12**, 108 (2012).
 - [23] L. Chang, X.-S. Jiang, S.-Y. Hua, C. Yang, J.-M. Wen, L. Jiang, G.-Y. Li, G.-Z. Wang, and M. Xiao, *Nat. Photon.* **8**, 524 (2014).
 - [24] B. Peng, Ş. K. Özdemir, F.-C. Lei, F. Monifi, M. Gianfreda, G.-L. Long, S.-H. Fan, F. Nori, C. M. Bender, and L. Yang, *Nat. Phys.* **10**, 394 (2014).
 - [25] C. Hang, G.-X. Huang, and V. V. Konotop, *Phys. Rev. Lett.* **110**, 083604 (2013).
 - [26] B. He, L. Yang, Z.-Y. Zhang, and M. Xiao, *Phys. Rev. A* **91**, 033830 (2015).
 - [27] B. He, S.-B. Yan, J. Wang, and M. Xiao, *Phys. Rev. A* **91**, 053832 (2015).
 - [28] X.-W. Xu and Y. Li, *Phys. Rev. A* **91**, 053854 (2015).
 - [29] Z. Lin, H. Ramezani, T. Eichelkraut, T. Kottos, H. Cao, and D. N. Christodoulides, *Phys. Rev. Lett.* **106**, 213901 (2011).

- [30] M. S. Kang, A. Butsch, and P. St. J. Russell, *Nat. Photon.* **5**, 549 (2011).
- [31] T. R. Zaman, X. Guo, and R. J. Ram, *Appl. Phys. Lett.* **90**, 023514 (2007).
- [32] A. E. Serebryannikov, *Phys. Rev. B* **80**, 155117 (2009).
- [33] S. F. Mingaleev and Y. S. Kivshar, *J. Opt. Soc. Am. B* **19**, 2241 (2002).
- [34] H. Zhou, K.-F. Zhou, W. Hu, Q. Guo, S. Lan, X.-S. Lin, and A. V. Gopal, *J. Appl. Phys.* **99**, 123111 (2006).
- [35] X.-S. Lin, J.-H. Yan, L.-J. Wu, and S. Lan, *Opt. Express* **16**, 20949 (2008).
- [36] A. Alberucci and G. Assanto, *Opt. Lett.* **33**, 1641 (2008).
- [37] S. Kuhr, W. Alt, D. Schrader, M. Müller, V. Gomer, and D. Meschede, *Science* **293**, 278 (2001).
- [38] H.-W. Cho, Y.-C. He, T. Peters, Y.-H. Chen, H.-C. Chen, S.-C. Lin, Y.-C. Lee, and I. A. Yu, *Opt. Express* **15**, 12114 (2007).
- [39] Y. Zhang, Y. Xue, G. Wang, C.-L. Cui, R. Wang, and J.-H. Wu, *Opt. Express* **19**, 2111 (2011).
- [40] M. Artoni, G. La Rocca, and F. Bassani, *Phys. Rev. E* **72**, 046604 (2005).
- [41] J. M. Bendickson, J. P. Dowling, and M. Scalora, *Phys. Rev. E* **53**, 4107 (1996).